Collective diffusion in an interacting one-dimensional lattice gas: Arbitrary interactions, activation energy, and nonequilibrium diffusion

Łukasz Badowski* and Magdalena A. Załuska-Kotur†
Institute of Physics, Polish Academy of Sciences, Al. Lotników 32/46, 02-668 Warsaw, Poland

Zbigniew W. Gortel‡
Department of Physics, University of Alberta, Edmonton, T6G 2J1 Alberta, Canada
(Received 28 April 2005; revised manuscript received 4 October 2005; published 13 December 2005)

Collective diffusion is investigated within the kinetic lattice gas model for a system of interacting particles in one dimension. Analytic relations between the collective diffusion coefficient, diffusion activation energy, the attempt frequency pre-exponential factor, vs the particle density for both attractive and repulsive particle-particle interactions of an arbitrary strength are derived using the recently proposed [Phys. Rev. B **70**, 125431 (2004)] variational method. The analytic results agree with results of Monte Carlo simulations within a broad range of temperatures. At low coverages for strongly repulsive interactions the activation energy is roughly equal to its value for the noninteracting system but around $\theta=0.5$ it decreases rapidly by more than strictly accounted for by adparticle-adparticle interactions. Only at significantly higher coverages it increases reaching the expected limiting value. Peaks in the coverage dependence of the effective attempt frequency (for both the repulsive and the attractive interactions) are interpreted to reflect peaks in the total number of microscopic configurations accessible to the system at a given coverage and temperature. It is argued that the method used in this work allows for making meaningful estimates of the diffusion coefficient for systems far from thermal equilibrium.

DOI: 10.1103/PhysRevB.72.245413 PACS number(s): 66.30.Pa, 02.50.Ga, 66.10.Cb, 68.43.Jk

I. INTRODUCTION

Kinetics of one-dimensional (1D) systems has recently become practically relevant as several experimentally studied and technologically important structures have 1D geometry. For example, static and dynamic properties of atoms confined in carbon nanotubes are now intensively studied;[1–3] diffusion of Au or Si atoms on top of Si(111)5×2-Au chain structure has one-dimensional character,[4,5] etc. Interactions in these 1D structures modify or even decide about the character of the system kinetics. In this work we calculate and analyze the collective diffusion coefficient that accounts for the rate of decay of long wavelength particle density fluctuations. When interactions between adsorbed atoms are present the collective diffusion becomes a complicated many-body problem,[6–12] but recently[13] an analytic method for calculating a density dependent diffusion coefficient for a system of interacting particles on a one-dimensional lattice was designed. Diffusion coefficient was extracted from a specific (referred to as diffusive) eigenvalue of a rate matrix describing kinetics of microscopic states of the system. Transitions between microstates are due to particle jumps from one site to another (provided such jump is allowed) and every such jump occurs at a specific jump rate. Following Ref. 13 we write master equations for the system in the form

$$\frac{\partial P_i}{\partial t}=\sum_{j\neq i}(w_{ij}P_j-w_{ji}P_i), \tag{1}$$

where P_i is a probability of finding the system in certain microscopic state i and w_{ij} is the transition rate from the microstate j to i. Together with the detailed balance condition these equations form a complete description of microscopic kinetics of the system. Each microstate is characterized by a position of an arbitrarily selected reference particle and by a microscopic configuration defined as a set of positions of all remaining particles with respect to the reference particle. The transition rates depend, in general, only on the initial and the final configuration. By imposing periodic boundary conditions and applying to this set of equations a lattice Fourier transform with respect to the position of the reference particle, a set of k-dependent rate equations is obtained. The indices of the k-dependent rate matrix $M_{i,j}(k)$ corresponding to this set refer to configurations rather than microstates. A matrix element $M_{ji}(k)$ for $i\neq j$ is related to a rate of the i to j transition. It may carry a k-dependent factor due to the phase difference between the sites involved in the jump. The diagonal matrix elements M_{ii} are related to jump rates out of the configuration i. See Eq. (16) later on. Generally, the matrix elements depend on k and a (the lattice constant). The diffusion coefficient is extracted from the diffusive eigenvalue of the matrix—defined as the eigenvalue that is proportional to $(ka)^2$ for $ka\ll1$. Any eigenvalue of the rate matrix may always be written as[13]

$$-\lambda=\frac{\sum_{i,j}\tilde{u}_jM_{ji}u_i}{\sum_i\tilde{u}_iu_i}=\frac{\sum_{i,j}\tilde{u}_jM_{ji}N(i)\tilde{u}_i^*}{\sum_i\tilde{u}_iN(i)\tilde{u}_i^*}, \tag{2}$$

where $\tilde{u}_i$ and u_i are the ith components of, respectively, the left and the right eigenvector of the rate matrix corresponding to this eigenvalue. The left and the right eigenvectors of the rate matrix are not conjugated since, in general, the rate

matrix is not Hermitian because transition rates between two configurations in opposite directions are different. They are, however, related to each other through $N(i)$—the probability of the configuration i in equilibrium[14]—and this relation was used to get the final result in Eq. (2). The denominator in Eq. (2) accounts for normalization. Approximations are needed for both the components of the left eigenvector $\tilde{u}$ as well as for $N(i)$'s in order to use Eq. (2) and, following Ref. 13, we seek the diffusive eigenvalue by evaluating

$$-\lambda \approx \frac{\sum_{i,j} \Phi_j^* M_{ij} N(i) \Phi_i}{\sum_i \Phi_i^* N(i) \Phi_i} \to -k^2 D, \tag{3}$$

in which components of the diffusive left eigenvector, $\tilde{u}_i$, are approximated with Φ_i^*, where

$$\Phi_i = 1 + e^{-ikan_1^i} + e^{-ikan_2^i} + \cdots + e^{-ikan_{N-1}^i}, \tag{4}$$

and the diffusion coefficient is extracted after the limit $ka \ll 1$ is taken, as indicated in Eq. (3). In Eq. (4), the term 1 at the beginning represents the reference particle, with respect to which the lattice Fourier transform was taken and $an_1^i, \ldots, an_{N-1}^i$ (n_j^i are integers) are distances of the remaining $N-1$ particles from the reference particle in the configuration i. In fact, the configuration i is fully specified by the set of integers $(n_1{}^i, \ldots, n_{N-1}{}^i)$.

It is worthwhile at this point to comment on the choice of $\Phi_i^*(k)$'s, given in Eq. (4), as candidates for $\tilde{u}_i$'s—components of the diffusive left eigenvector of the rate matrix. It was shown in Ref. 13 that Φ_i^*'s are the components of the exact diffusive left eigenvector of the rate matrix for a noninteracting lattice gas with site blocking for which all allowed particle jumps occur at the same rate. Choosing Φ_i's to evaluate $-\lambda$ for a system with interactions, accounting for them effectively only in the rate matrix $M_{i,j}$ and the probabilities $N(i)$, is an approximation similar in its spirit to the variational approach approximation in quantum mechanics where a "guessed" wave function approximating true ground state wave function is used to evaluate the expectation value of the exact Hamiltonian. We are here on a less certain ground than in quantum mechanics, however, because $-\lambda$ evaluated for the non-Hermitian rate matrix $M_{i,j}$ is not necessarily bounded from below by the true eigenvalue. Also, there exist quite intuitively clear guidelines helping to select physically acceptable candidates for the ground state wave functions in quantum mechanics. Such guidelines have not been worked out yet to help with the choice of the components of the diffusive eigenvector of the rate matrix. The only condition which we are aware of is that all components of the left diffusive eigenvector must have the same $k \to 0$ limit with corrections linear in k. It assures that the evaluated approximate $\lambda(k)$ vanishes quadratically with k in this limit—the condition which the diffusive eigenvalue must satisfy. Consequently, $\Phi_i(k)$ given in Eq. (4) is merely the simplest and most obvious choice. Applying our approach to investigate diffusion in a two-dimensional lattice gas with strongly repulsive interactions,[15] we have found it necessary to go beyond a direct two-dimensional generalization of Eq. (4) while selecting the variational candidate for the diffusive eigenvector.

A collective diffusion coefficient was evaluated from Eqs. (3) and (4) in Ref. 13 for a one-dimensional lattice gas with strong repulsive interactions and for a case in which the interactions weakly modify the jump rates between the sites. Recently, the method was successfully applied to investigate collective diffusion in a two-dimensional lattice gas on a square lattice in which strong repulsive interactions induce structural organization of the gas into a $c(2\times 2)$ phase.[15] For strongly repulsive interactions one could restrict summations in the numerator and in the denominator in Eq. (3) to include only a few types of configurations that are most probable in equilibrium. The main technical obstacle, which so far has prevented applying the method to cases with arbitrary short-range interactions, is the necessity of dealing with a much wider class of configurations than for strong repulsion, while keeping finite the system size and the number of particles in it. In such cases, summations over configurations lead to multiple and strongly interdependent summations over occupied lattice sites, and the task quickly becomes intractable. It is a goal of this work to modify the method to be able to deal with arbitrary interactions in the one-dimensional case. In principle, the modification is simple: while dealing with summations in Eq. (3) one opens the system by removing restrictions imposed by its finiteness and introduces at the same time a Lagrange multiplier to fix, on average, the particle density. In other words, rather than dealing with the numerator and the denominator in Eq. (3) for a closed system, one evaluates their "grand canonical" counterparts.

In Sec. II the theoretical method is formulated and analytic expressions for the grand canonical denominator, numerator, and for the Lagrange multiplier are obtained. They lead, in Sec. II C, to an approximate expression for the density dependent collective diffusion coefficient, $D(\theta)$, which is confronted with the numerical simulation data in Sec. III. Analytic results for $D(\theta)$ are used in Sec. IV to discuss features of the particle density dependence of the activation energy and of the pre-exponential frequency factor commonly used to parametrize the diffusion coefficient. This allows for a connection to be made between the results of the present work and the results obtained in Ref. 13. In Sec. V we propose a method of dealing with diffusion far from equilibrium in certain cases, and Sec. VI is devoted to a short summary of the paper. Some technical details not required for understanding the results are placed in two Appendixes.

II. THEORY

We stay within the one-dimensional model, as defined in Ref. 13, of a lattice with identical potential wells with minima at adsorption sites separated by a. Periodic boundary conditions are accounted for by distributing all sites along the circumference of a circle. Only the nearest neighbor interactions between particles determine the particle jump rates. Therefore, there are only four different types of jumps (and four different rates) $w_{ij}=W,\Gamma,R$, and T as shown here,

$$\cdots\circ\bullet\rightarrow\circ\circ\cdots, \quad W,$$

$$\cdots\bullet\bullet\rightarrow\circ\circ\cdots, \quad \Gamma,$$

$$\cdots\circ\bullet\rightarrow\circ\bullet\cdots, \quad R,$$

$$\cdots\bullet\bullet\rightarrow\circ\bullet\cdots, \quad T. \tag{5}$$

Jumps of a free particle occur at a rate W and all other rates are determined by repulsive or attractive interactions between the particles.

For N particles in the system there are N bonds between them (if the periodic boundary condition is taken into account). A bond longer than a is referred to as a broken bond. Otherwise, when its length is exactly a, it is referred to as a saturated one. The number of broken bonds in a given configuration is an integer s between 1 and N (corresponding, respectively, to the maximum $N-1$ and the minimum 0 saturated bonds). Jumps occurring at rates W or T do not change the number of saturated or broken bonds. A jump at a rate Γ breaks a saturated bond, while a jump at a rate R saturates a broken bond so, if J is the interaction energy, then the ratio $p=\Gamma/R$ has the following property:

$$p = \frac{\Gamma}{R} = e^{\beta J}, \quad \begin{array}{l} p>1 \quad \text{(repulsion)}, \\ p=1 \quad \text{(no interactions)}, \\ p<1 \quad \text{(attraction)}, \end{array} \tag{6}$$

where β is the inverse of temperature (times the Boltzmann constant).

The interaction energy of a configuration with s broken bonds is $(N-s)J$. Consequently, the equilibrium probability $N(i)$ of a configuration i with s_i broken bonds is proportional to p^{s_i}. In fact, we can set $N(i)\equiv p^{s_i}$ in Eq. (3) because any factor normalizing the probability cancels out between the numerator and the denominator there. Therefore,

$$-\lambda \approx \frac{\sum_{i,j} \Phi_j^* M_{ji} p^{s_i} \Phi_i}{\sum_i \Phi_i^* p^{s_i} \Phi_i} = \frac{X}{Y}. \tag{7}$$

A. Denominator

With Φ_i given in Eq. (4) the product $(\Phi_i)^*\Phi_i$ in the denominator Eq. (7),

$$Y = \sum_i \Phi_i^* p^{s_i} \Phi_i, \tag{8}$$

is a sum of exponentials $e^{ika(n_j^i - n_{j'}^i)}$ with relative positions of all pairs of particles $[(j,j')$, including $j=j']$ in a particular configuration i appearing in the exponent. The summation over configurations in Eq. (8) can be rearranged into a more manageable form. The idea is to consider patterns like

$$\cdots\bullet\cdots \delta \text{ sites} \cdots\bullet\cdots ,$$

in which two selected particles are separated by δ sites (occupied or empty), determine how many times it occurs, multiply that number by a proper probability factor p^s and then sum over all possible distances δ. To proceed with this program we divide the entire system of N particles into two parts, referred to as the δ-section and the environment, as shown in Fig. 1.

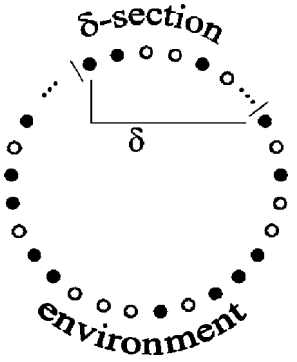

FIG. 1. Dividing the system into sections.

The number of particles, holes, and broken bonds in the δ-section are denoted by n_δ, h_δ, and s_δ, respectively, while n_ϵ, h_ϵ, and s_ϵ denote the corresponding numbers in the environment. Note that $\delta = n_\delta + h_\delta$.

Any of the two subsystems (δ-section or environment) containing h holes (at least one) and n particles (at least one) with s broken bonds (at least one) can be realized in the following number of ways:

$$B(n,h,s) = \binom{n}{s}\binom{h-1}{s-1} \quad \text{for } n,h,s \geqslant 1, \tag{9}$$

assuming that first site in the subsystem is occupied. In Eq. (9) the number of possible partitions of n particles into s clusters $\binom{n-1}{s-1}$, is multiplied by the number of partitions of h holes into s clusters $\binom{h-1}{s-1}$, and then all possible positions of the reference particle are summed up resulting effectively in an extra factor n/s. In cases of no holes ($h=0$) or of no particles ($n=0$) in the subsystem the number of possibilities is 1.

For the entire system with specified N and H the number of configurations corresponding to a given set of six parameters $n_\delta, h_\delta, s_\delta$ and $n_\epsilon, h_\epsilon, s_\epsilon$ is equal to a product $B(n_\delta, h_\delta, s_\delta) B(n_\epsilon, h_\epsilon, s_\epsilon)$ and the probability factor is p^S where $S = s_\delta + s_\epsilon$. Summation over configurations in Eq. (8) becomes a summation over all six parameters but the number of summations is reduced at least by two due to the restrictions,

$$H - h_\delta = h_\epsilon,$$

$$N - n_\delta = n_\epsilon,$$

imposed by the total number of particles and holes in the system. The number of broken bonds does not exceed the number of particles or holes, whichever is smaller. This must be reflected in the upper limits in summations over s_δ and s_ϵ. Cases in which all sites in either the δ-section or environment are occupied must be treated separately. The result for Y is

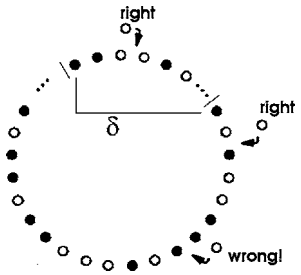

FIG. 2. Proper and improper hole injection procedure.

$$Y(N,H,p,k) = \sum_{n_\delta=1}^{N-1} \sum_{h_\delta=1}^{H-1} \sum_{s_\epsilon=1}^{\min\{h_\epsilon,n_\epsilon\}} \sum_{s_\delta=1}^{\min\{h_\delta,n_\delta\}} p^S B_\delta B_\epsilon e^{ika(h_\delta+n_\delta)} + \sum_{n_\epsilon=1}^{N-1} \sum_{s_\epsilon=1}^{\min\{H,n_\epsilon\}} p^{s_\epsilon} B(n_\epsilon,H,s_\epsilon) e^{ikan_\delta} + \sum_{n_\delta=1}^{N-1} \sum_{s_\delta=1}^{\min\{H,n_\delta\}} p^{s_\delta} B(n_\delta,H,s_\delta) e^{ika(H+n_\delta)} + \sum_{s_\epsilon=1}^{\min\{H,N\}} p^{s_\epsilon} \binom{H-1}{s_\epsilon-1}\binom{N}{s_\epsilon}, \quad (10)$$

where $B_\delta \equiv B(n_\delta,h_\delta,s_\delta)$, $B_\epsilon \equiv B(n_\epsilon,h_\epsilon,s_\epsilon)$, and $S=s_\delta+s_\epsilon$ in the first term on the right-hand side. For the sake of the development to follow it is more convenient to consider Y to be a function of N and H rather than that of N and $L=N+H$. The first contribution on the right-hand side of Eq. (10), the most general one, is due to all configurations with at least one broken bond within each subsystem, implying that each subsystem contains at least one particle and at least one hole. The first site is always occupied. The second contribution is due to all configurations with all sites of the δ-sections being occupied, and the third contribution is due to those in which all sites of the environments are fully occupied. Finally, the last contribution corresponds to configurations with $\delta=0$ (no δ-sections)—here all configurations of the environment are counted.

The sums [as given in Eq. (10)] are not easy to evaluate and lead to a complicated result involving generalized hypergeometric functions. To get a simpler result an approximation is needed to decouple the subsystems and to enable summing over the variables of each of them separately. Then, the variables for the individual subsystems can be let go to infinity, i.e., the restrictions due to the definite numbers of either particles or holes (but not both at the same time) can be relaxed.

Consider particular configuration of the system containing N particles and H holes distributed among L sites of a one-dimensional lattice with L sites forming clusters of particles and holes. Clusters of particles—containing at least one particle—are separated with clusters of holes (also containing at least one hole). Broken bonds are placed at the edges of particle clusters. Adding (injecting) an extra hole to a cluster of holes does not change the number of broken bonds (i.e., does not change the interaction energy) but leads to a new configuration (see Fig. 2) of the system with unchanged number of particles, unchanged number of broken bonds but larger number of holes. Applying this repeatedly to all hole clusters, one produces a wide range of configurations with the same number of particles and broken bonds.

Injecting holes to the original system (while keeping the number of particles fixed at N) implies that the number of sites, $L=H+N$, also increases and the particle and the hole densities are no longer fixed. To keep the particle density N/L at a predetermined value θ, a Lagrange multiplier r is introduced and its value is fixed in such a way that the mean value of the ratio H/N is equal to $(1-\theta)/\theta$. Of course, this is the same as requesting that the mean number of holes is equal to its actual value because N is fixed in the procedure. This procedure is, in fact, very similar to that used in standard statistical mechanics when a transition is made from the canonical to grand canonical ensemble: N and H are analogues, respectively, of the fixed volume and the particle number, p plays a role of temperature, and the Lagrange multiplier r is an analogue of fugacity (and will be referred to as such in what follows). In the noninteracting system it is proportional to the density of holes, i.e., $r=1-\theta$ for $p=1$. We note in passing that the opening of the system may alternatively be accomplished by injecting particles into particle clusters rather than holes into the hole clusters—the roles played by particles and holes are then reversed. The results of both approaches should be the same.

The result of this approach is that the actual denominator Y, given in Eq. (10), is replaced with its "grand canonical" counterpart $\bar{Y}$ which depends now on r rather than H,

$$\bar{Y}(N,r,p,k) = \sum_{n_\delta=1}^{N-1} \sum_{s_\epsilon=1}^{n_\epsilon} \sum_{s_\delta=1}^{n_\delta} \sum_{h_\epsilon=s_\epsilon}^{\infty} \sum_{h_\delta=s_\delta}^{\infty} p^S r^H B_\delta B_\epsilon \cos(ka\delta) + \sum_{n_\delta=1}^{N-1} \sum_{s_\epsilon=1}^{n_\epsilon} \sum_{H=s_\epsilon}^{\infty} p^S r^H B(n_\epsilon,H,s_\epsilon)\cos(kan_\delta) + \sum_{n_\delta=1}^{N-1} \sum_{s_\delta=1}^{n_\delta} \sum_{H=s_\delta}^{\infty} p^S r^H B(n_\delta,H,s_\delta)\cos[ka(n_\delta+H)] + \sum_{s_\epsilon=1}^{N} \sum_{h_\epsilon=s_\epsilon}^{\infty} p^{s_\epsilon} r^H B(N,h_\epsilon,s_\epsilon). \quad (11)$$

The trigonometric functions group conjugated terms of the original sum in Eq. (10)). The sums in Eq. (11) are evaluated in Appendix A. The result is

$$\bar{Y} = \left(\frac{pr}{1-r}+1\right)^N \frac{pr[(p-1)r^2+1]}{|(p-1)[e^{iak}(1-r)+1]r+1|^2}. \quad (12)$$

It depends on N, the fugacity r, the interaction parameter p, and on ka.

The fugacity r must be determined by the condition fixing the mean number of holes

$$H = r\frac{\partial}{\partial r}\ln\left[\sum_{n=1}^{N}\sum_{s=1}^{n}\sum_{h=s}^{\infty} p^s r^h \binom{h-1}{s-1}\binom{n}{s}\right]. \quad (13)$$

Its evaluation is easy and in the thermodynamic limit we get

$$\frac{pr}{(1-r)[(p-1)r+1]} = \frac{H}{N} = \frac{1-\theta}{\theta}. \tag{14}$$

Among two solutions of this equation for r as a function of p and θ the relevant one is for which $0 \leqslant r \leqslant 1$. For the noninteracting case ($p=1$) we have $r=1-\theta$ and the $r(\theta)$ lines lie above (below) the $r=1-\theta$ line for all attractive (repulsive) interactions.

B. Numerator

The evaluation of the numerator in Eq. (7) is, in general, a problem similar to that discussed above for the denominator. One must evaluate

$$X = \sum_{ij} \Phi_j^* M_{ji} p^{s_i} \Phi_i. \tag{15}$$

It can be dealt with exactly like it was in Ref. 13, as summarized in what follows. First, matrix elements of the rate matrix are

$$M_{ji}(k) = F_{ji}(k) w_{ji} \quad \text{for } i \neq j, \quad M_{ii} = -\sum_{\langle l \rangle_i} w_{li}. \tag{16}$$

Here, $F_{ji}(k)=1$ for all transitions $i \to j$ in which the hopping particle is not the reference particle. When the reference particle jumps, then the distances of all remaining particles from it change by $+a$ or $-a$ depending on the direction of the jump and then $F_{ij}(k)=\exp(\pm ika)$. This phase factor arises when the lattice Fourier transform of original rate equations is taken. The rates w_{ji} are equal to zero for configurations i and j differing in positions of more than one atom. Otherwise, they are equal W, Γ, R, or T depending on the immediate environment of the hopping particle. Consequently, the summation over $\langle l \rangle_i$ is restricted to such configurations l which can be reached from the configuration i by a hopping of a single particle between nearest neighbor sites. Using Eq. (16) we get the following expression for the numerator

$$X = \sum_{ji}^{\text{no rep}} w_{ji} p^{s_i} |F_{ji}\Phi_i - \Phi_j|^2, \tag{17}$$

where s_i is the number of broken bonds in the configuration i. The detailed balance condition $w_{ij}p^{s_j} = w_{ji}p^{s_i}$ has been used so the summation over ij accounts for both, $i \to j$ and $j \to i$ transitions. To avoid double counting of transitions each pair of configurations with $w_{ji} \neq 0$ appears in the summation only once, as indicated by "no rep" above Σ. It is easy to check that $|F_{ji}\Phi_i - \Phi_j|^2 = \sin^2(ka)$ for all such pairs. The actual value of w_{ji} depends only on the occupation state of the nearest neighborhood of the jumping particle. It is, therefore, convenient to introduce an active cell which consists of four sites, a pair of sites between which the particle jumps plus one site at each side of the pair. There are four types of such cells. Each one corresponds to one of the transition rates $w_{ji} = W, \Gamma, R$, and T and they are shown in Eq. (5). The occupation pattern in the environment outside the active cell is arbitrary. Each particular type of the active cell (i.e., each of the four possible values of w_{ij}) brings into X in Eq. (17) a contribution proportional to the number of possible configurations of the environment outside the active cell. Its evaluation is a very similar task to the one presented in the case of the denominator. The evaluation is now even easier because the active cell has always constant and finite length, $\delta=4$.

Opening the system by injecting holes into the environment and introducing the fugacity r permits us to avoid complications due to the restrictions imposed by a finite number of particles and holes. Details are given in Appendix B. The grand canonical counterpart $\bar{X}$ of the numerator X is a sum of contributions due to each type of particle jumps listed in Eq. (5):

$$\bar{X}(N,r,p,k) = (\bar{X}_T + \bar{X}_\Gamma + \bar{X}_R + \bar{X}_W)\sin^2\left(\frac{ka}{2}\right). \tag{18}$$

With the detailed balance condition $\Gamma = pR$ the contributions $\bar{X}_R$ and $\bar{X}_\Gamma$ are identical. All contributions are listed in Eqs. (B3)–(B5). They depend on p, N, and r and the latter must be determined by solving Eq. (14).

C. Diffusion coefficient

The collective diffusion coefficient is evaluated as a $ka \to 0$ limit of $\bar{X}/k^2\bar{Y}$ [cf. Eq. (3)]. Collecting the results for $\bar{Y}$ and all contributions to $\bar{X}$ we get

$$D(\theta) = \frac{pr^2[(p-1)(r-2)r-1]^2}{[(p-1)r+1]^2[(p-1)r^2+1]} \times \left[W + 2R\frac{1-r}{r} + \frac{T}{p}\left(\frac{1-r}{r}\right)^2\right]a^2, \tag{19}$$

with the θ dependence entering through r obtained from Eq. (14). The term proportional to R accounts for both the R and the Γ type transitions (thus a factor 2 in front of it).

It is worthwhile to note here two points. (i) Equation (19) exhibits the particle-hole symmetry, it is invariant upon the simultaneous $W \leftrightarrow T$ and $\theta \leftrightarrow (1-\theta)$ replacements [the latter must be also made in Eq. (14) at the same time]. This means that the same result would be obtained by injecting particles rather than holes into the system. (ii) It is well known in standard statistical mechanics that the results obtained within canonical and grand canonical approaches are identical in the thermodynamic limit of a large system. It is, thus, expected that the expression for the diffusion coefficient obtained from the ratio $\bar{X}/\bar{Y}$ should be in this limit identical with the expression which would be obtained in this limit from the ratio X/Y (a significantly more difficult procedure). It is reassuring to realize in this context that for the case without interactions, i.e., for $p=1$, and $T=R=\Gamma=W$, Eq. (19) yields $D(\theta)=Wa^2$, i.e., the exact coverage independent collective diffusion coefficient.

III. NUMERICAL RESULTS

We compare here the analytic results of our model with the results of numerical Monte Carlo simulations. We have used a simple Monte Carlo method for dynamics and a variant of the Boltzmann-Matano method to obtain the density

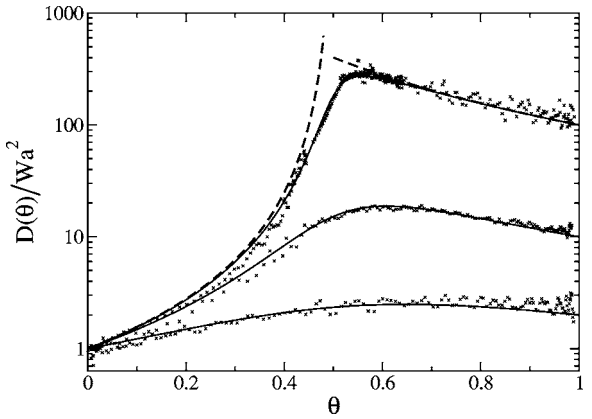

FIG. 3. Density dependence of the collective diffusion coefficient for repulsive particle-particle interactions. Points, MC simulation results solid lines, theoretical results from Eq. (19); dashed lines, analytic results from Ref. 13. The interaction parameters (counting from top to bottom) are $p=100$, 10, 2.

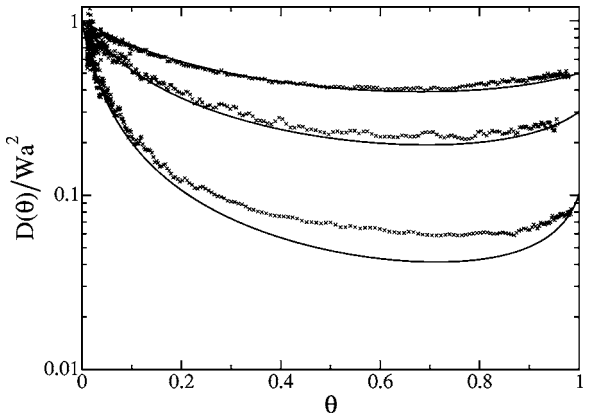

FIG. 4. The same as in Fig. 3 but for the attractive interactions. Parameters $p=0.5$, 0.3, 0.1, counting from top to bottom.

dependence of the collective diffusion coefficient.[16–18] The initial steplike density profile was chosen with particles occupying all N lattice sites within a certain interval with all the remaining sites being empty. The particles were free to jump with rates determined according to the interaction model. Jump rates selected were $W=R, \Gamma=T=pW$. The results have been averaged over 10^6 MC steps and were smoothed using running-on averages of different range depending on the slope of the curve.

For the repulsive interactions the numerical results are presented in Fig. 3. The low density limit of the normalized diffusion coefficient is fixed, $D(\theta=0)/Wa^2=1$, and the high density limit depends on the interaction parameter p. The analytic results are plotted using Eq. (19). We see that the analytic results fit very well the numerical ones, and that for this particular set of parameters they agree also quite well with the analytic results of the earlier, simpler version of our model[13] (dashed line) for both strong ($p=100$, 10) and weak ($p=2$) repulsive interactions. Note, however, that in contrast to the latter, the present version of the model has no discontinuity at $\theta=0.5$ for strongly repulsive interactions.

In Fig. 4 the MC simulation results are confronted with the predictions of Eq. (19) for attractive interactions. The fit to the simulation data is quite good except in the immediate vicinity of $\theta=0.5$. It can be either due to the approximations used in the theory or due to difficulties with the analysis of the computer simulation data. The one-dimensional system does not change its ordering through the phase transition but it has a tendency to cluster particles into strongly and weakly occupied islands. Systems that cluster are very difficult to analyze numerically and, in particular, it is difficult in this case to extract accurately values of the diffusion coefficient from the simulation data. In this situation it is surprising that the agreement between our simple analytic formula and the results of the MC simulations of diffusion in such inhomogeneous state of the system is as good as observed in Fig. 4.

IV. ACTIVATION ENERGY AND ATTEMPT FREQUENCY

In most of the experimental studies the following parametrization of diffusion coefficient is introduced:

$$D(\theta,\beta) = \nu a^2 e^{-\beta E_A(\theta)}, \tag{20}$$

containing parameters which can be fit to parameters measured in other experiments. Here, E_A is referred to as an activation energy and ν is known as an attempt frequency. The parametrization written above extracts temperature dependence explicitly. The temperature in our calculations enters via rates that we use in the model. The equilibrium weight $p=\exp(\beta J)$ gives $p \gg 1$ for low temperature systems with repulsion ($J>0$) and $p \ll 1$ for low temperature systems with attraction ($J<0$). Temperature decides also about dynamical processes in the system, through $W=W_0 \exp(-\beta V)$, and relations between other rates. W_0 is a temperature and interaction independent attempt frequency for an isolated particle, and V is an interaction independent barrier height between the adsorption sites. We extract the interaction dependent part of the diffusion coefficient by considering the ratio

$$\frac{D(\theta)}{D(0)} = \frac{D(\theta)}{Wa^2} = \frac{\nu}{W_0} e^{-\beta[E_A(\theta)-V]}, \tag{21}$$

and analyzing its density dependence for the interacting system.

The activation energy is a parameter that provides an information on the effective potential energy of a particle during the evolution of the system. Its density-dependent part $E_A(\theta)-V$ depends on the interaction constant J in the system Hamiltonian. The prefactor $\nu(\theta)$ is the effective interaction-dependent frequency with which a particle tries to jump out of its potential well. In other words, E_A is modified by interaction change in the energy barrier encountered by a particle leaving an "average" adsorption site and ν accounts for the "average" dynamic properties of particles, also modified by the interactions. Of course, in real situations $E_A(\theta)$ and $\nu(\theta)$ depend on temperature so Eq. (20) is only an approximate parametrization of the temperature dependence. It is possible to extract both, the attempt frequency $\nu(\theta)$ and the activation energy $E_A(\theta)-V$ from the analytic expression for $D(\theta)$, given in Eq. (19). Changing p keeping J fixed means varying the temperature, for the repulsive interactions' higher temperatures correspond to smaller p's (always larger than 1)

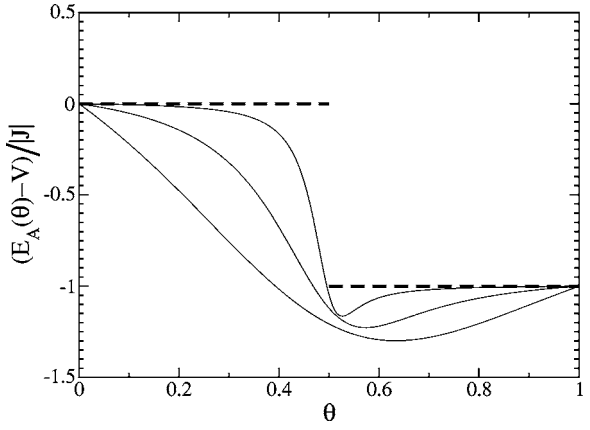

FIG. 5. Interaction-induced correction to the activation energy as a function of the particle density for repulsive interactions for $W=R$ and $\Gamma=T$. Counting from the topmost curve down, $p=100, p=10$, and $p=2$, corresponding to the lowest, intermediate, and the highest temperature, respectively. Dashed line, the result from the simplified version of the model in Ref. 13.

while for the attractive ones higher temperatures correspond to larger p's (always smaller than 1). Results, for several temperatures (i.e., p's), are plotted in Figs. 5 and 6 for the repulsive interactions, and in Figs. 7 and 8 for the attractive ones.

It can be seen that both variables E_A as well as ν depend on temperature. The character of their density dependence is qualitatively similar at all temperatures. Upon increasing p, i.e., lowering the temperature, this dependence approaches the limit corresponding to the results of the simplified model of Ref. 13. In this limit the diffusion coefficient is equal to $D(\theta)=W_0a^2e^{-\beta V}/(1-2\theta)^2$ for $\theta<0.5$ and to $D(\theta)=W_0a^2e^{-\beta(V-J)}/\theta^2$ for $\theta>0.5$. In the simplified model the interaction induced modification of the activation energy is equal to 0 for densities below $\theta=0.5$ and to $-J$ above it (dashed line in Fig. 5). The effective attempt frequency is in this limiting case proportional to $(1-2\theta)^{-2}$ for $\theta<0.5$ and to θ^{-2} for $\theta>0.5$ (dashed line in Fig. 6). In the present model

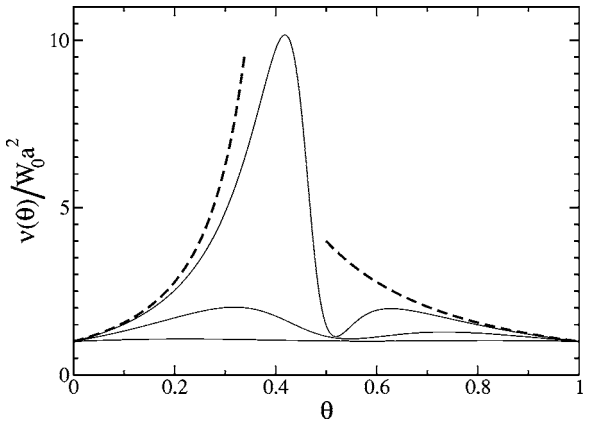

FIG. 6. Effective attempt frequency as a function of the particle density for the repulsive interactions. The parameters p are the same as in Fig. 5. The lowest temperature ($p=100$) corresponds to the topmost curve. Dashed line, the result from a simplified version of the model in Ref. 13.

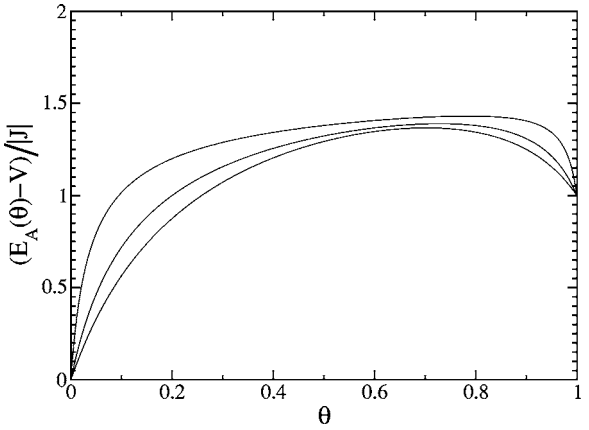

FIG. 7. The same as in Fig. 5 but for the attractive interactions for $W=R$ and $\Gamma=T$. Counting from the topmost curve down, $p=0.1$, 0.3, and 0.5 corresponding to the highest, intermediate, and the lowest temperature, respectively.

both parameters reveal an interesting behavior around $\theta=0.5$ for repulsive interactions. The activation energy decreases rapidly around $\theta=0.5$. This is not surprising because the limiting case approximation predicts it too. More interesting is a small dip observed immediately above $\theta=0.5$. Here the activation energy is lowered by more than J—coming from single interaction and this feature is absent from the limiting case approximation.

The attempt frequency approaches a "bare" value W_0 at $\theta=0.5$. Even more interesting behavior occurs to the left and to the right of this point. A clear maximum is observed for densities around $\theta=0.4$ and somewhat less pronounced maximum in the vicinity of $\theta=0.6$. As stated before, the attempt frequency accounts for the dynamical properties of the system. At different densities the number of microscopic configurations that are visited at a given temperature is different. It is relatively low at $\theta=0.5$ but rises considerably for densities higher or lower than $\theta=0.5$. The number of possible deconstructions increases away from $\theta=0.5$, which is reflected in a larger attempt frequency. Thus the attempt frequency contains information about the size of space of effectively accessible configurations.

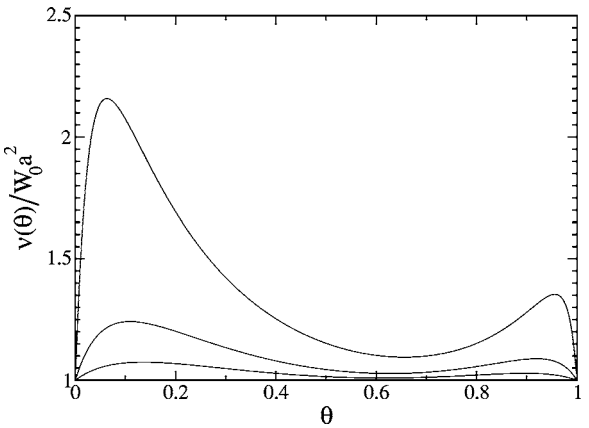

FIG. 8. The same as in Fig. 6 but for the attractive interactions for $W=R$ and $\Gamma=T$. The parameters p are the same as in Fig. 7. The lowest temperature ($p=0.1$) corresponds to the topmost curve.

The density dependence of the activation energy and of the attempt frequency for the attractive interactions is plotted in Figs. 7 and 8. We see that with lowering temperature the activation energy $(E_A-V)/|J|$ increases.

The attempt frequency probes the size of the effectively accessible portion of the configuration phase space and, again, shows regions where the system has the largest freedom. The maxima of the attempt frequency appear close to $\theta=0.5$ for the repulsive interactions (Fig. 6) but for the attractive interactions (Fig. 8) they occur closer to $\theta=0$ and $\theta=1$. This difference reflects a difference in the basic properties of the phase space available to the system's different kinds of interactions. Although in one dimension no phase transition occurs, positions of the observed maxima occur, however, at positions at which phase transitions in similar two-dimensional (2D) systems take place, a coverage interval over which an ordered phase in 2D occurs is wider for the repulsive interactions than it is for the attractive ones.

V. DIFFUSION FAR FROM EQUILIBRIUM

Using the approach presented in this work we may attempt to estimate the decay rate of long wavelength density fluctuations for the system far from equilibrium. This is relevant when the system is prepared in an initial state that significantly differs from the equilibrium state at the actual temperature at which the temporal evolution occurs. One can, for example, equilibrate the system at a high temperature T_h and then suddenly quench it substantially down to T_q and follow then the approach towards equilibrium. We may identify the rate of decay towards equilibrium, $1/\tau$, of fluctuations corresponding to the wave vector k over a short time window around t with an "expectation value" of the rate matrix M_{ji} in the corresponding to k state $u_i(t)$ of the system at t,

$$-\frac{1}{\tau}=\frac{\sum_{i,j}\tilde{u}_j(t)M_{ji}u_i(t)}{\sum_i \tilde{u}_i(t)u_i(t)}, \tag{22}$$

In particular, evaluating $1/\tau$ at $t=0$ [i.e., using the initial state of the system represented by $u_i(0)$] we get an estimate of the initial rate of decay. If the system is prepared in such a way that the rate of decay is proportional to k^2,

$$\tau^{-1}=\tilde{D}a^2k^2 \tag{23}$$

then the parameter $\tilde{D}$ may be understood as the far-from-equilibrium chemical diffusion coefficient. Strictly speaking, only very special initial states of the system result in the initial decay rate with the property (23) so, formally, $\tilde{D}$ is not as universal quantity describing properties of the system as the standard diffusion coefficient is. The latter describes the final approach to equilibrium after all transients have already died out and, consequently, it does not depend on the initial state of the system.

If the system is prepared at a sufficiently high temperature then, at $t=0$ all microstates of the system are equally likely, i.e., $p=1$ and the appropriate vector $u_i(0)$ is equal to $\Phi_i(k)$ given in Eq. (4). The resulting rate of decay was in fact already evaluated in a different context in Ref. 13. The result for $\tilde{D}$ is

$$\tilde{D}=W+2(\Gamma-R-W)\theta(1-\theta)+(T-W)\theta^2, \tag{24}$$

where W,T,R, and Γ are the hopping rates appropriate to the "quenched" temperature T_q at which the initial time evolution is followed. The activation energy parameter corresponding to $\tilde{D}$ (whatever it physically means) is in Fig. 9 compared with the equilibrium activation energy for strongly repulsive interactions and the temperature corresponding to $p=100$. We see that for $\theta<0.5$ the equilibrium activation energy is about two orders of magnitude higher than that corresponding to the far from equilibrium diffusion. This is reminiscent of the experimentally observed relation[19] between the activation energies for ordered (equilibrium) and disordered (far form equilibrium) systems. Note that slightly above $\theta=0.5$ the equilibrium activation energy drops below the far from equilibrium one but as θ approaches 1 both activation energies become the same.

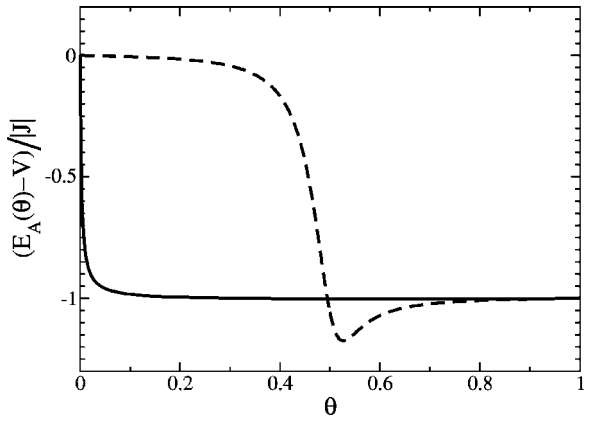

FIG. 9. Interaction-induced correction to the activation energy as a function of the particle density for repulsive interactions for $W=R,\Gamma=T$, and $p=100$ for the far from equilibrium (continuous line), and for the equilibrium (dashed line) diffusion coefficient.

VI. SUMMARY

We have applied and generalized in this work the recently developed[13] approach to chemical diffusion in one-dimensional lattice gas system of interacting particles to account for both repulsive and attractive interactions of arbitrary magnitude. Analytical results for the density (coverage) dependence of the collective diffusion coefficient agree very well with the results of computer simulations.

Unphysical discontinuity of the diffusion coefficient at $\theta=0.5$, predicted for strongly repulsive interactions in Ref. 13, is now removed and a nontrivial dependence of both the activation energy and the diffusion pre-exponential factor (attempt frequency) is obtained. It is shown that in this case the results of Ref. 13 correspond to the zero temperature limit of the presently obtained results.

For strongly repulsive interactions and/or at low temperatures the activation energy remains approximately constant

with increasing density, assuming at moderate coverages a value appropriate for the system without interactions, but it drops rapidly down by more than the particle-particle interaction energy when one-half of the lattice sites get occupied (i.e., at 1/2 coverage). It gradually approaches the value expected for diffusion of independent holes with further increase of density. The drop is less rapid at higher temperatures and/or for weaker repulsive interactions but its magnitude is always larger than the interaction energy. Pronounced maxima of the attempt frequency at densities slightly below and slightly above 1/2 coverage occur when the number of accessible microscopic configurations of the system is the largest. For the attractive interactions the density dependence is smoother than for repulsion but the interpretation remains essentially the same.

An attempt was also made to parametrize collective diffusion for systems far from thermal equilibrium. For systems prepared at high temperatures and subsequently quenched, the activation energy of the initial (far from equilibrium) diffusion coefficient is, for repulsive interactions and low coverages, much lower than that of the equilibrium coefficient, with both merging each other for $\theta > 0.5$.

Our approach is akin to the variational approach in standard quantum mechanics; the diffusive eigenvalue is approximated by an "expectation value" of the rate matrix, using a variational guess for the appropriate eigenvector. In contrast to quantum mechanics we do not have here a benefit of either the variational principle (assuring that the approximated eigenvalue is not smaller than its true value) or of the intuitions which we usually have concerning the shape of the ground state wave functions. In this situation the variational choice in Eq. (4) for the left diffusive eigenvector of the rate matrix is the simplest but not necessarily the best choice. Being the exact eigenvector of the rate matrix for the lattice gas without interactions (except for hard core repulsion), it necessarily has all the properties required for the eigenvalue to be proportional to k^2 in the long wavelength limit. The matter of an optimal variational choice of the eigenvector that would partially take into account the actual interactions requires further investigation of the formal properties of the diffusive eigenvectors. These properties would serve then as a guide in searches for more appropriate variational candidates. In fact, in our own investigations of diffusion in the interacting lattice gas in two dimensions with strong nearest neighbor interactions[15] we have considered a variational choice of the diffusive eigenvector going beyond simple 2D generalization of Eq. (4). The choice was dictated by considering several special and limiting cases.

Only a lattice gas in one dimension is a subject of this work. In a separate publication[15] results of our investigations of collective diffusion in a two-dimensional lattice gas with strong repulsive interactions will be presented for the density range within which the gas is organized into a $c(2\times 2)$ structural phase. Similarly as in Ref. 13 for 1D the diffusion coefficient experiences a discontinuity at $\theta=0.5$. Similarly as in Ref. 13, it is an artifact caused by limiting considerations to relatively few types of the most likely configurations accessible to the system. Removing the discontinuities as well as generalization to cases with arbitrary interactions requires, similarly as in this work, considering much broader class of configurations and using the grand canonical approximation scheme. Work in this direction is in progress.

ACKNOWLEDGMENTS

This work was partially supported by research grants from the Polish State Committee for Scientific Research (Grant No. 2 P03B 048 24 - MZK) and from the National Sciences and Engineering Research Council (NSERC) of Canada (Z.W.G.).

APPENDIX A

We provide here a few guidelines through calculations leading from Eq. (11) to Eq. (12). The use of two identities[20]

$$\sum_{x=y}^{\infty} r^{x-y}\binom{x}{y} = \frac{(1-r)^{-y}}{1-r}, \tag{A1}$$

$$\sum_{y=0}^{x} r^{y}\binom{x}{y} = (r+1)^{x}, \tag{A2}$$

is repeatedly made in it.

It is important to notice that, while h_δ and h_ϵ vary independently of each other, n_δ and n_ϵ are not mutually independent because the system has a fixed number of particles $n_\delta + n_\epsilon$. Therefore we sum over numbers of holes first [using Eq. (A1)]. The sum over numbers of broken bonds [with help of Eq. (A2)] and over particles is relatively easy once the summation over h_δ and h_ϵ is done. Let us take the first part of the expression (11). Two inner sums are independent of each other—they lead to

$$\bar{Y}_1(s_\delta, s_\epsilon, n_\delta) = \frac{(pr)^{s_\delta+s_\epsilon}}{(1-r)^{s_\epsilon}}\left(\frac{e^{-iak(n_\delta+s_\delta)}}{(1-e^{-iak}r)^{s_\delta}} + \frac{e^{iak(n_\delta+s_\delta)}}{(1-e^{iak}r)^{s_\delta}}\right), \tag{A3}$$

where the subscript 1 refers to the first term of Eq. (11). The other two sums result in

$$\bar{Y}_1(n_\delta) = \left[\left(\frac{pr}{1-r}+1\right)^{N-n_\delta} - 1\right]\left(e^{-iakn_\delta}\left(\frac{pr}{e^{iak}-r}+1\right)^{n_\delta} + e^{iakn_\delta}\left\{\left[p\left(\frac{1}{1-e^{ika}r}-1\right)+1\right]^{n_\delta} - 1\right\} - e^{-iakn_\delta}\right), \tag{A4}$$

which summed over n_δ gives

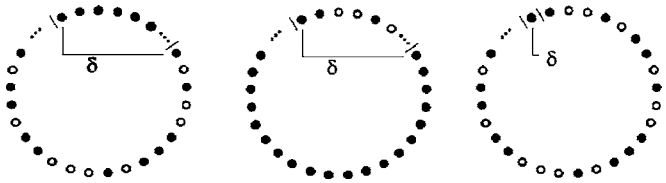

FIG. 10. Special cases in the denominator in Eqs. (10) and (11). From left to right, Cases 2, 3, and 4.

$$\bar{Y}_1 = \left(\frac{pr}{1-r}+1\right)^N \frac{pr(1-r)[(p-1)r+1]}{|(1-r)-e^{-iak}[(p-1)r+1]|^2} \times \left(\frac{(p^2r^2(r-2)-(2-3p)r(r-1)^2)}{|(p-1)r(1-r)+e^{-iak}[(p-1)r+1]|^2} - \frac{[(p-1)r+1]^2 2\cos(ak)}{|(p-1)r(1-r)+e^{-iak}[(p-1)r+1]|^2}\right) + \frac{pr^2(p-2)+2\cos(ak)}{|e^{-iak}(p-1)r+(r+1)-e^{iak}|^2}. \quad \text{(A5)}$$

One must perform similar summations for every remaining three special case terms in Eq. (11) as described below. In Fig. 1 a typical configuration of the system is shown. It consists of a δ-section and an environment, and corresponds to terms in the innermost sums in the first term of the denominator (10). Diagrams corresponding to three other cases are shown in Fig. 10.

Case 2 corresponds to a situation when the entire δ-section is completely filled with particles so all broken bonds are present in the environment. Holes may thus be injected only outside the δ-section (compare it with Fig. 2) and do not contribute to the length δ. The result is

$$\bar{Y}_2 = 1 - \left(\frac{pr}{1-r}+1\right)^N \frac{(1-r)-((p-1)r+1)2\cos(ak)}{|(1-r)-e^{-iak}((p-1)r+1)|^2}. \quad \text{(A6)}$$

Case 3 is exactly opposite to Case 2—the environment is filled with particles and has no holes, which can only be injected between broken bonds within the δ-section. Note that the number of particles in the system is fixed so the length of the environment is restricted by the total number of particles minus one. We get

$$\bar{Y}_3 = -\frac{pr^2(p-2)+2\cos(ak)}{|e^{-iak}r(p-1)+(r+1)-e^{iak}|^2}. \quad \text{(A7)}$$

Case 4 is the simplest one. Here, δ-section is reduced to one particle only. This case appears also in the calculation of the r parameter. We get

$$\bar{Y}_4 = \left(\frac{pr}{1-r}+1\right)^N - 1. \quad \text{(A8)}$$

Adding $\bar{Y}_1$ through $\bar{Y}_4$ results in the expression for Y given in Eq. (12).

APPENDIX B

In the numerator there are four possible types of active cells corresponding to four jump types. Generally speaking for each of them we repeat a procedure which was used in Appendix A for the denominator, but keep s_δ, n_δ, and h_δ fixed at their values appropriate to a given cell type. The entire numerator is a sum of contributions from different types of active cells $X=\bar{X}_T+\bar{X}_W+\bar{X}_\Gamma+\bar{X}_R$.

The T-type active cell has three particles and one hole, and one broken bond is located within the cell. Since the δ section is fixed (and equal to the active cell), the summation runs over the environment configurations only. One possibility is a typical environment with a certain number of hole clusters to which additional holes may be injected (as pictured in Fig. 2). For $h_\epsilon \neq 0$ in the environment we get

$$\bar{X}_T^{h_\epsilon} = Tpr\left[\left(\frac{pr}{1-r}+1\right)^{N-2} - 1\right], \quad \text{(B1)}$$

where the superscript h_ϵ means that the result (B1) is valid for the case with $h_\epsilon \neq 0$ holes in the environment. The other case occurs when no hole is present in the environment (note that it is still a reasonable regime since one hole is present within the active cell). In such a case we get

$$\bar{X}_T^0 = Tpr. \quad \text{(B2)}$$

Adding both results leads to the following T-type active cell contribution to the numerator

$$\bar{X}_T = Tpr\left(\frac{pr}{1-r}+1\right)^{N-2}. \quad \text{(B3)}$$

For W-type active cell we get a similar result, only the number of holes and particles in the active cell is now different,

$$\bar{X}_W = W\frac{p^2r^3}{(1-p)[r(p-1)+1]}\left(\frac{pr}{1-r}+1\right)^{N-1}. \quad \text{(B4)}$$

In contrast to the former two, the Γ- and R-type active cell cannot be easily written as a sum of a δ-section and an environment. The basic cell in both cases has particle at one end and hole at the other, whereas δ-section has particles at both ends. Instead we can write the sum of all configurations of environment for Γ-type cell as a difference of configuration number for the appropriate three particle δ-section and four particle δ-section. Due to the detailed balance condition, we can calculate only one of the Γ-type contributions and get the other one using the substitution $\Gamma = pR$. We get

$$\bar{X}_\Gamma \equiv \bar{X}_R = R\frac{(r-1)r^2p^2}{[(p-1)r+1]^2}\left(\frac{pr}{1-r}+1\right)^{N-1}. \quad \text{(B5)}$$

*Electronic address: lukasz.badowski@ifpan.edu.pl
†Electronic address: zalum@ifpan.edu.pl
‡Electronic address: gortel@phys.ualberta.ca

[1] W. Teizer, R. B. Hallock, E. Dujardin, and T. W. Ebbesen, Phys. Rev. Lett. **82**, 5305 (1999); **84**, 1844 (2000).
[2] M. Hodak and L. A. Girifalco, Phys. Rev. B **64**, 035407 (2001).
[3] V. Meunier, J. Kephart, C. Roland, and J. Bernholc, Phys. Rev. Lett. **88** 075506 (2002).
[4] T. Hasegawa and S. Hosoki, Phys. Rev. B **54**, 10300 (1996).
[5] A. Kirakosian, R. Bennewitz, F. J. Himpsel, and L. W. Bruch,

Phys. Rev. B **67**, 205412 (2003).
[6] D. A. Reed and G. Ehrlich, Surf. Sci. **102**, 588 (1981).
[7] R. Gomer, Rep. Prog. Phys. **53**, 917 (1990).
[8] A. Danani, R. Ferrando, E. Scalas, and M. Torri, Int. J. Mod. Phys. B **11**, 2217 (1997).
[9] T. Ala-Nissila, R. Ferrando, and S. C. Ying, Adv. Phys. **51**, 949 (2002).
[10] H. J. Kreuzer, in *Diffusion at Interfaces: Microscopic Concepts*, edited by M. Grunze, H. J. Kreuzer, and J. J. Weimar, Springer Series in Surface Sciences Vol. 12 (Springer, New York, 1988), p. 63.
[11] H. J. Kreuzer and J. Zhang, Appl. Phys. A **A51**, 183 (1990).
[12] H. J. Kreuzer, J. Chem. Soc., Faraday Trans. **86**, 1299 (1990).
[13] Z. W. Gortel and M. A. Załuska-Kotur, Phys. Rev. B **70**, 125431 (2004).
[14] H. J. Kreuzer and Z. W. Gortel, *Physisorption Kinetics*, Springer Series in Surface Sciences Vol. 1 (Springer, New York, 1986), Chap. 3.
[15] M. A. Załuska-Kotur and Z. W. Gortel, Phys. Rev. B (to be published).
[16] M. A. Załuska-Kotur, S. Krukowski, and Ł. A. Turski, Surf. Sci. **441**, 320 (1999).
[17] M. A. Załuska-Kotur, S. Krukowski, Z. Romanowski, and Ł. A. Turski, Surf. Sci. **457**, 357 (2000).
[18] M. E. Glicksman, *Diffusion in Solids* (Wiley, New York, 2000), Chap. 11.
[19] M. Tringides, Prog. Surf. Sci. **53**, 225 (1996).
[20] I. S. Gradshteyn and I. M. Ryzhik, *Table of Integrals, Series, and Products* (Academic, New York, 1980).